The 0.7 anomaly in one-dimensional hole quantum wires

2008 J. Phys.: Condens. Matter 20 164205

(http://iopscience.iop.org/0953-8984/20/16/164205)

J. Phys.: Condens. Matter **20** (2008) 164205 (8pp) doi:10.1088/0953-8984/20/16/164205

The 0.7 anomaly in one-dimensional hole quantum wires

A R Hamilton[1], R Danneau[1,2], O Klochan[1], W R Clarke[1], A P Micolich[1], L H Ho[1], M Y Simmons[1], D A Ritchie[3], M Pepper[3], K Muraki[4] and Y Hirayama[4,5]

[1] School of Physics, University of New South Wales, Sydney, NSW 2052, Australia
[2] Low Temperature Laboratory, Helsinki University of Technology, Espoo, Finland
[3] Cavendish Laboratory, University of Cambridge, J J Thompson Avenue, Cambridge CB3 0HE, UK
[4] NTT Basic Research Laboratories, NTT Corporation, 3-1 Morinosato Wakamiya, Atsugi, Kanagawa 243-0198, Japan
[5] Department of Physics, Tohoku University, 6-3 Aramaki aza Aoba, Aobaku Sendai, Miyagi 980-8578, Japan

E-mail: Alex.Hamilton@unsw.edu.au

Received 18 December 2007, in final form 23 February 2008
Published 1 April 2008
Online at stacks.iop.org/JPhysCM/20/164205

Abstract

In this paper we study the anomalous 0.7 structure in high quality ballistic one-dimensional hole systems. Hole systems are of interest because of their large effective mass, strong spin–orbit coupling, as well as having spin 3/2 compared to spin 1/2 for electrons. We observe remarkably clean conductance quantization in a variety of different samples, and a strong feature at $\sim 0.7 \times 2e^2/h$, which shows a similar temperature and density dependence to the 0.7 feature observed in electron systems. In contrast to the case for electrons, the strong spin–orbit coupling results in an anisotropic Zeeman splitting, which we use to probe the 0.7 feature and the associated zero-bias anomaly. Our results indicate that the 0.7 feature and the zero-bias anomaly are related, and both are suppressed by spin polarization. These results place valuable constraints on models of the microscopic origins of the 0.7 feature.

(Some figures in this article are in colour only in the electronic version)

1. Introduction

One-dimensional (1D) electron quantum wires and quantum point contacts (QPCs) have been extensively studied for the past 20 years [1, 2]. While the quantization of the 1D ballistic conductance $g = i \times 2e^2/h$ (where i is an integer) is well established, the origin of an unexpected feature at $\sim 0.7 \times 2e^2/h$ remains an outstanding anomaly. The so-called '0.7 structure' was first studied in detail by Thomas *et al* [3], although it can be seen in the first measurements of 1D electron systems from 1988 [1]. The 0.7 structure is often observed in electron point contacts, and is believed to arise from electron–electron interactions and spin. However despite extensive study the microscopic origins of the 0.7 structure remain elusive, with explanations including phonon scattering [4], 1D Wigner crystallization, enhanced scattering, and the Kondo effect [5, 6].

Hole systems are of interest because of their large effective mass and strong spin–orbit coupling. The large hole mass, $m^* = 0.2$–$0.4m_e$, quenches the kinetic energy and enhances many body interaction effects, which are parameterized by $r_s \propto m^*/\sqrt{n_s}$. In contrast to 2D electron systems which are limited to $r_s \lesssim 5$, in 2D hole systems $r_s \gg 10$ can easily be achieved. For example $r_s = 1.7$ for 2D electrons at a typical density of 10^{11} cm^{-2}, whereas for holes r_s is closer to 10. The strong spin–orbit coupling makes it possible to manipulate the hole spin with an applied electric field, and the total angular momentum $j = 3/2$ gives low dimensional hole systems a much richer spin physics than their electron counterparts [7]. However to date there have been comparatively few studies of hole quantum wires, primarily due to the difficulties in fabricating stable high mobility devices [8–10]. In this work we present data from high quality spin-3/2 hole quantum wires, focussing on the 0.7 structure and how it compares to

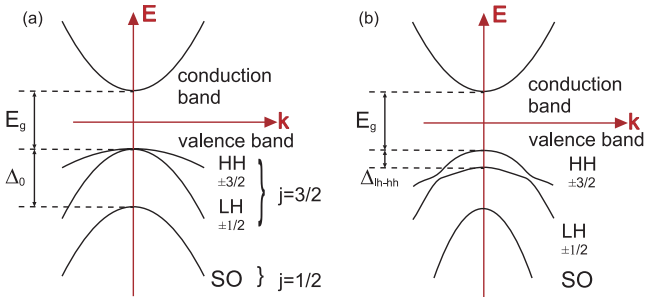

Figure 1. (a) Schematic band diagram for bulk GaAs, showing the split-off (SO), light-hole (LH), heavy-hole (HH), and conduction bands. (b) Schematic band diagram for a 2D hole system where the HH–LH degeneracy is lifted at $k = 0$ due to the 2D confinement.

that observed in spin-1/2 electron quantum wires. We address the following questions:

- Is there a 0.7 structure in hole quantum wires?
- How do the strong hole–hole interactions affect the 0.7 structure?
- The single particle 1D hole subbands have an anisotropic Zeeman splitting, which we use to probe the 0.7 structure: if it is related to spin, it should show a similar anisotropy.

2. Hole bandstructure and sample fabrication

2.1. An overview of the hole bandstructure

The GaAs valence band structure is significantly more complex than the simple parabolic conduction band for electrons, as shown in figure 1(a) for bulk GaAs [7]. Conduction band electrons originate from s-like $l = 0$ states, and are not affected by the $l.s$ spin–orbit interaction to leading order. Electrons have intrinsic angular momentum (spin) $\hbar/2$, with a quantized projection in any direction of $m_S = \pm\hbar/2$. In contrast the valence band states are p-like, with $l = 1$. The spin–orbit interaction lifts the six-fold degeneracy of the valence band states at $k = 0$, leading to a splitting Δ_0 between the valence band states with total angular momentum $j = 3/2$ (the light and heavy holes) and those with $j = 1/2$ (the split-off band). Holes from the two uppermost valence band branches have an intrinsic angular momentum (spin) $3\hbar/2$, and have 4 projections $m_j = \pm 3\hbar/2$ (heavy holes, HH) and $m_j = \pm\hbar/2$ (light holes, LH).

Confining the holes to a 2D system lifts the light-hole heavy-hole degeneracy at $k = 0$, as depicted in figure 1(b), so that the HH ($m_J = \pm 3/2$) band becomes the lowest energy hole band. The bandstructure becomes quite complex at higher energies, due to an anticrossing of the LH and HH bands. This anticrossing comes about because the hole mass is anisotropic: the effective mass of the $m_j = \pm 3/2$ 'heavy' holes is lighter for motion in the 2D plane than that of the $m_j = \pm 1/2$ 'light' holes. Fortunately in 2D hole systems we are far from this anticrossing: the Fermi energy is small ($E_F \sim 1$ meV), significantly less than the light-hole heavy-hole splitting ($\Delta_{lh-hh} \sim 10$ meV), so that only the heavy-hole band is occupied. A nice treatment of the 2D hole bandstructure is given in the authoritative book by Winkler [7].

The response of holes to an external magnetic field is also different to electrons. Spin-1/2 electrons behave like a dipole in a magnetic field, with a magnetic moment μ_B and a Zeeman splitting of the energy levels given by $g\mu_B B$. In contrast spin-3/2 holes are described by dipole, quadrupole and octupole moments [11]. This has many implications—for example the spin splitting of hole states is highly anisotropic, depending on the orientation of the magnetic field.

When confined to one-dimensional quantum wires the electronic and spin properties of holes become very sensitive to the geometry of the quantum wire and the characteristic length scales [12–14]. For example, we can examine the nature of the band-edge states at $k = 0$ in two limiting cases: in a very narrow quantum wire, such as a self assembled nanowire, the lowest energy hole state changes character, with the $m_j = 1/2$ 'light'-hole band becoming lower in energy than the $m_j = 3/2$ 'heavy'-hole band (the opposite of the 2D case). The other limit is where the 2D confinement from the quantum well (~10 nm in our case) is stronger than the lateral quantum wire confinement (~100 nm in our quantum wires). In this case the ground state remains predominantly $m_j = 3/2$ HH-like, although there are strong effects of the 1D confinement on the electronic and spin properties of the holes in the quantum wire.

One of the key advantages of studying 1D hole systems is that we study the depopulation of the 1D subbands, and therefore are primarily examining the behaviour at the band-edge where $k = 0$ in the direction of motion. This is in contrast to transport measurements of 2D or 3D systems, which probe the hole states at finite k. This is advantageous since the effect of an applied magnetic field on states with finite k, in the presence of strong spin–orbit coupling and 1D confinement, is highly complex. Thus studying 1D hole systems allows us to probe the hole states, and their response to a magnetic field, in a manner that is difficult to do in higher dimensions.

2.2. Sample fabrication

Hole quantum wires were fabricated from high quality two-dimensional hole systems formed in GaAs/AlGaAs heterostructures grown on (311)A GaAs substrates. The first heterostructure, shown in figure 2(a), is an 'induced' single heterojunction in which the holes are introduced by a negative bias applied to a degenerately doped p^+-GaAs gate electrode, instead of by modulation doping the AlGaAs layer [15]. This approach avoids unwanted scattering from remote ionized impurities, and allows the 2D hole density to be varied over a wide range. The holes are confined in a triangular potential well, with densities from 1.6×10^{10} to 1.9×10^{11} cm^{-2} and mobilities up to 700 000 cm^2 V^{-1} s^{-1}. To define a quantum wire the p^+-GaAs layer is divided into three electrically separate gates using electron beam lithography and a shallow etch, as indicated in figure 2(b), with the quantum wire aligned along the [$\bar{2}$33] direction [16]. The hole density in the 1D quantum wire and the 2D reservoirs on the left and right of it are controlled with a negative bias applied to the central top-gate. At the same time, a positive bias applied to

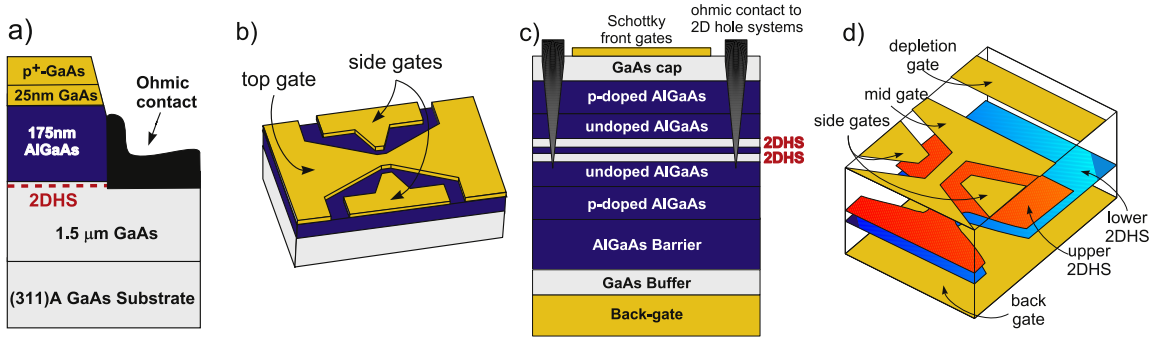

Figure 2. Schematic of the heterostructures used to make the two hole quantum wires discussed in this paper. (a) The 'undoped' heterostructure R165 in which a high mobility 2D hole system is formed by applying a negative bias to the p-GaAs gate. (b) Schematic of the three p-GaAs gates used to define a quantum wire at the GaAs/AlGaAs heterojunction. (c) The double quantum well heterostructure T483, in which holes are supplied by modulation doping. The top and bottom quantum wells are separated by a thick AlGaAs barrier to prevent inter-well tunnelling. (d) Schematic of the gate layouts used to define the quantum wires. The two side-gates control the wire width, and a central mid-gate controls the hole density in the upper quantum wire. The back-gate is used to control the density in the lower quantum wire, and can be used to deplete the lower quantum wire completely so that the upper quantum wire can be measured independently. The measurements presented here are from the upper quantum wire.

the two side-gates controls the effective width of the 1D wire formed 200 nm below the gate[6].

The second type of heterostructure is a modulation doped double quantum well in which two sheets of high mobility holes are formed in 20 nm wide GaAs quantum wells separated by a 30 nm AlGaAs barrier (figure 2(c)). The barrier is sufficiently thick that there is no tunnelling between the two 2D hole layers. The as-grown hole densities in the two wells are 1×10^{11} cm^{-2} with peak mobilities in excess of 10^6 cm^2 V^{-1} s^{-1}. Ohmic contacts are made to both 2D hole systems in parallel, and an overall back-gate can be used to control the hole density in the lower quantum well. Two parallel quantum wires are defined along the [$\bar{2}$33] direction by Schottky gates, as shown in figure 2(d), using electron beam lithography and thermal evaporation techniques [17]. A combination of front and back-gate biases allows the transport properties of the top or bottom quantum wire to be measured in isolation. A positive bias applied to the two side-gates defines the one-dimensional channels in the two quantum wells. The central top-gate is used to control the density in the upper quantum wire, and the back-gate controls the density in the lower quantum wire. Thus the top quantum wire can be measured in isolation by depleting the lower wire with the back-gate. In addition a separate depletion gate can be used to stop the current flow in the top quantum well, even when it is not depleted. This allows the lower quantum wire to be measured without having to deplete the upper wire [17, 18], and can be used to measure the compressibility of 1D systems [18]. All measurements were performed using low frequency ac lock-in techniques at the base temperature of a dilution refrigerator (25 mK), unless otherwise stated.

[6] Note that it is not possible to independently control the carrier density or quantum wire width with a single gate. However a combination of gates, such as employed here, can be used to achieve this (cf [24]).

3. Ballistic transport and the 0.7 structure in hole quantum wires

3.1. Ballistic transport in hole quantum wires

We begin by showing typical examples of the clean conductance quantization observed in hole quantum wires fabricated from both quantum wells and single heterojunctions. The inset to figure 3(a) shows an electron micrograph of the Schottky gates used to define the quantum wire on the modulation doped double quantum well device [17]. A central mid-gate (MG) controls the hole density in the wire, while the two side-gates (SG) are used to adjust the wire width. In this paper we only show data from measurements of the upper quantum wire, biasing the back-gate to $V_{BG} = 2.5$ V to deplete the lower quantum well. The data in figure 3(a) shows the conductance of the upper quantum wire as a function of the side-gate bias. A constant series resistance due to the ohmic contacts, wiring and external apparatus has been subtracted from the two-terminal measurements. We observe up to 11 clean conductance plateaux and a strong 0.7 structure [17], without any of the resonances or artefacts that have hampered previous studies of lower mobility hole devices [8, 10]. Similar data is obtained for the quantum wire in the lower quantum well (not shown) [19, 20]. The device and data are highly robust, exhibiting the same characteristics across multiple thermal cycles.

The inset to figure 3(b) shows an electron micrograph of the gates used to define the quantum wire on the undoped single heterojunction [16]. The gate structure and operation is similar to that of the double quantum well heterostructure: the side-gates are used to pinch-off the quantum wire, while the overall top-gate (TG) controls the hole density in the quantum wire as well as in the 2D reservoirs. The peak mobility in this device structure is slightly lower than in the modulation doped structure, but is high enough that the device shows 7 clean conductance steps, with additional structure below the

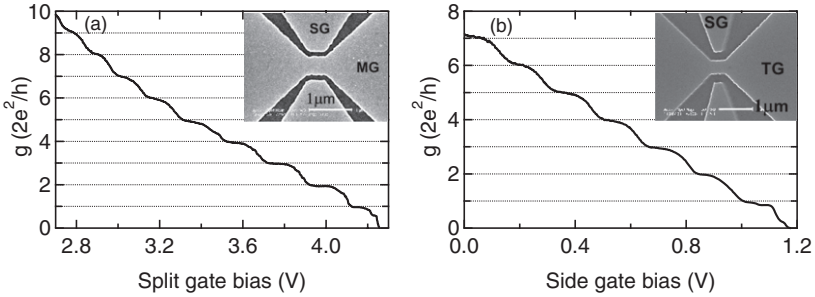

Figure 3. Conductance quantization in two hole quantum wires: (a) The quantum wire fabricated on the T483 modulation doped double quantum well heterostructure. The data shows the conductance of the upper quantum wire as a function of the side-gate bias, with $V_{BG} = 2.5$ V and $V_{MG} = -0.225$ V. The inset shows an electron micrograph of the Schottky gate pattern; the light regions are the metal gates. (b) The quantum wire fabricated on the R165 undoped single heterojunction, with $V_{TG} = -0.48$ V. The inset shows the gate pattern; the light regions are the degenerately doped p-GaAs gates.

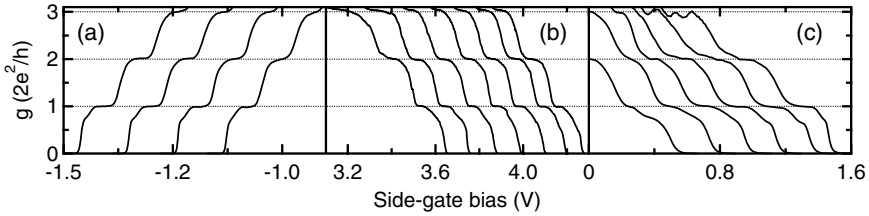

Figure 4. Density dependence of the '0.7 structure' in electron and hole samples. (a) Evolution of the 0.7 structure in an electron quantum wire as the density of the 2D electron gas is varied from 1.8 to 2.4×10^{11} cm^{-2}. (b) Similar data for the upper hole quantum wire in sample T483 as the carrier density is increased with the mid-gate bias. V_{MG} is stepped from -0.175 V (on the left) to -0.475 V (on the right) in 0.05 V increments. (c) Data for a hole quantum wire in the single heterojunction R165, as the 2D hole density is varied with the mid-gate bias from 9.9×10^{10} to 1.35×10^{11} cm^{-2} in steps of 7×10^{9} cm^{-2}.

first plateau. These devices are exceptionally stable, without the hysteresis or instabilities that occur in most modulation doped devices.

3.2. Density dependence of the 0.7 structure

One of the main differences between electron and hole quantum wires is the much larger effective interaction strength r_s in holes, which might be expected to have implications for the 0.7 structure. To test the effects of interactions we have studied the density dependence of the 0.7 structure in both electron and hole systems. In 1D electron systems there are conflicting reports about the density dependence: some studies find the '0.7 structure' moves closer to $0.5 \times 2e^2/h$ as the density is decreased [21], others find that it moves towards $0.5 \times 2e^2/h$ as the density is increased [22], and some studies show both trends [23].

As a reference, figure 4(a) shows the evolution of the 0.7 structure in an electron quantum wire as the 2D electron density is varied with a back-gate bias [24]. Each trace corresponds to a different 2D electron density, from 1.8 to 2.4×10^{11} cm^{-2} ($r_s = 1.3$–1.1). The data show a weak dependence of the 0.7 structure on the 2D density, with the feature becoming more visible and moving to slightly higher conductance as the electron density is increased and the 1D confining potential becomes stronger due to the increasingly negative side-gate bias (leftmost traces).

Figures 4(b) and (c) show the evolution of the 0.7 structure in hole quantum wires with varying hole density. Figure 4(c) shows data from a single heterojunction hole QPC similar to that shown in figure 1(b). The top-gate bias alters the 2D hole density p_{2D} from 9.9×10^{10} cm^{-2} to 1.35×10^{11} cm^{-2} (left to right, corresponding to $r_s = 13$–11), with the 1D confinement being stronger at the higher hole densities. Similar to the data from electrons in figure 4(a) the 0.7 structure moves to slightly higher conductance as the carrier density is increased (rightmost traces). Figure 4(b) shows the evolution of the 0.7 structure in the modulation doped T483 quantum wire, as the mid-gate bias is used to increase the hole density in the 1D channel (from left to right). In this device there is no clear variation of the 0.7 structure with V_{MG}; if anything it appears to get weaker as V_{MG} is increased.

Overall, for both electron and hole quantum wires there seems to be no clear variation in the visibility of the 0.7 structure, and conductance at which it occurs, with carrier density. Furthermore despite r_s in the electron and hole samples differing by a factor of 5 or more, the data in figures 4(a) and (c) look similar. This suggests that the 0.7 structure may be more sensitive to the potential landscape and/or the disorder environment than to the strength of the interactions.

3.3. Temperature dependence of the 0.7 structure

Figure 5 shows the temperature dependence of the ballistic transport in the undoped and the modulation doped quantum wire devices. Both show the same behaviour: increasing

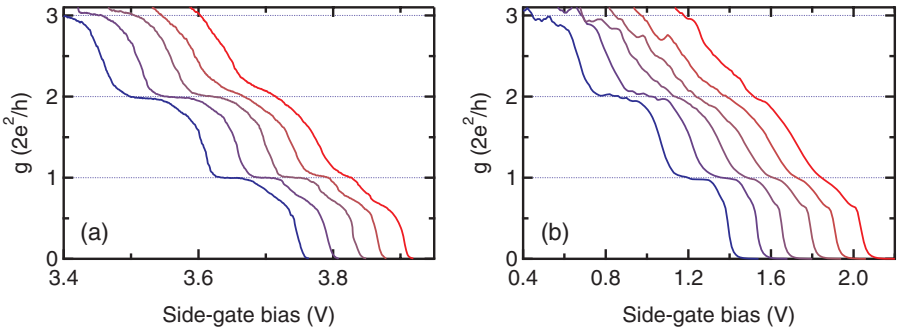

Figure 5. Temperature dependence of the 0.7 structure in hole quantum wires. (a) For the quantum well sample T483 with $V_{MG} = -0.225$ V and $T = 20$, 200, 320, 550, and 650 mK. (b) For the R165 single heterojunction, at $V_{TG} = -0.40$ V ($p_{2D} = 1.35 \times 10^{11}$ cm^{-2}) for $T = 25$, 175, 370, 515, 620, and 715 mK. Curves have been offset horizontally for clarity.

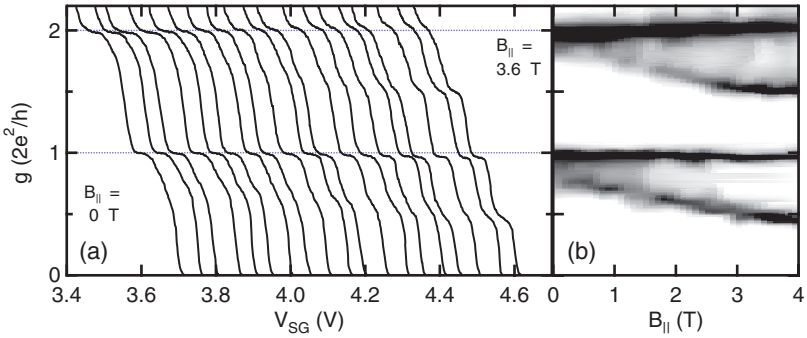

Figure 6. (a) Conductance of the T483 quantum wire as a function of side-gate voltage V_{SG}, for different values of the magnetic field applied parallel to the wire (along [$\bar{2}$33]). Traces have been offset for clarity, and $B_\parallel$ is increased in 0.2 T steps from 0 to 3.6 T. (b) Greyscale image of the data, showing the evolution of the conductance plateaus as a function of the applied magnetic field. The colour axis is the transconductance $\partial g/\partial V_{SG}$, with dark regions denoting the conductance plateaus.

the temperature rapidly weakens the single particle 1D conductance plateaux, with the plateaux washed out by $T \sim 700$ mK. This strong temperature dependence is consistent with measurements of the 1D subband spacing in these devices, which gives $\Delta E \sim 0.2$–0.4 meV for the first few subbands, significantly lower than the 1.5–3 meV found in comparable electron systems [25]. The small subband spacings measured in our hole wires are consistent with the large hole mass, since $\Delta E \propto 1/m^*$ and $m_h^* \approx 5m_e^*$.

In contrast to the single particle plateaus, the '0.7 structure' becomes *more* prominent as the temperature is increased, and moves closer to $0.5 \times 2e^2/h$. Analogous structure is also seen in the higher 1D subbands, for example at $\sim 1.7 \times 2e^2/h$ in figure 5(a). Both of these observations are consistent with the behaviour seen in 1D electron systems.

4. Anisotropic response of the 0.7 structure and zero bias anomaly to an in-plane magnetic field

So far the data for hole quantum wires looks remarkably similar to that for electron quantum wires, despite the much stronger hole–hole interactions. We now turn to the effects of an in-plane magnetic field applied parallel to the heterojunction, which are quite different for electrons and holes.

4.1. Evolution of the 0.7 structure with in-plane magnetic field

For hole quantum wires the Zeeman splitting of the 1D subbands is highly dependent on the orientation of the magnetic field, due to the strong spin–orbit coupling in the valence band. For quantum wires fabricated on (311)A heterostructures the interplay of the confinement potential and the crystal anisotropy means that the Zeeman splitting is much larger when the magnetic field is applied parallel to the quantum wire (along [$\bar{2}$33]), than when it applied perpendicular to the quantum wire (along [01$\bar{1}$]) [26]. This is quite different to 1D electrons, where the Zeeman splitting has been shown to be isotropic and independent of the direction of the in-plane field [3]. We use this extreme anisotropy of the spin splitting in 1D holes to probe the 0.7 structure: if it is related to spin, then it too should show an anisotropic response to an in-plane magnetic field.

Figure 6(a) shows the conductance of the T483 quantum wire for different magnetic fields applied parallel to the wire. At zero magnetic field the conductance is quantized in units of $2e^2/h$, with a clear feature at $0.7 \times 2e^2/h$. The magnetic field rapidly lifts the spin degeneracy of the hole subbands: at $B = 2$ T the spin-split conductance plateaus can clearly be resolved, and by $B = 3.6$ T they are as strong as the $i \times 2e^2/h$ plateaus. By 7 T the spin splitting of the 1D subbands is comparable to the subband spacing ΔE, and 1D subbands with

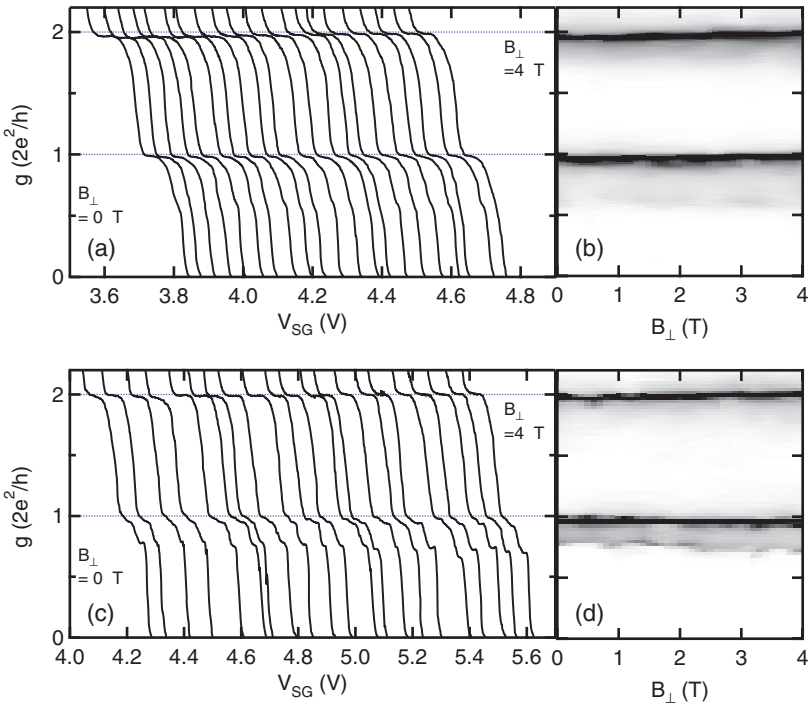

Figure 7. (a) Conductance of the T483 quantum wire as a function of side-gate voltage V_{SG}, for different values of the magnetic field applied perpendicular to the wire (along $[01\bar{1}]$). Traces have been offset for clarity, and $B_\perp$ is increased in 0.2 T steps from 0 to 4 T. (b) Greyscale image of the data, showing the evolution of the conductance plateaus as a function of the applied magnetic field. The colour axis is the transconductance $\partial g/\partial V_{SG}$, with dark regions denoting the conductance plateaus. (c), (d) show measurements repeated after the device has been thermally cycled to room temperature and back to base temperature.

different spin orientations cross each other. Figure 6(b) shows a graphical representation of the evolution of the conductance plateaus as a function of parallel magnetic field. The dark regions represent the conductance plateaus. At $B_\parallel = 0$ there are plateaus at $1 \times 2e^2/h$ and $2 \times 2e^2/h$, as well as a clear feature at $0.7 \times 2e^2/h$ that rapidly evolves to $0.5 \times 2e^2/h$ as the magnetic field is increased.

The behaviour of the hole quantum wire is quite different when the in-plane magnetic field is applied perpendicular to the wire, along the $[01\bar{1}]$ direction. In order to study this the sample was thermally cycled and reoriented with respect to the magnet axis. To verify that the properties of the quantum wire were not affected by this thermal cycling, the 1D subband spacings were measured after each cool-down, and were found to be constant to within our experimental accuracy of 5%. Figure 7 shows the conductance of the quantum wire for different perpendicular magnetic fields. In contrast to the measurements in a parallel magnetic field, the perpendicular field appears to have almost no effect on the 1D subbands. The integer plateaus at $1 \times 2e^2/h$ and $2 \times 2e^2/h$ at $B_\perp = 0$ show no signs of spin splitting by $B_\perp = 4$ T, whereas they are fully spin resolved in a parallel magnetic field of $B_\parallel = 2$ T.[7] The lack of spin splitting can be seen very clearly in figure 7(b), which shows the same graphical representation of the evolution of the conductance plateaus as depicted in figure 6(b). We thermally cycled the device and repeated these measurements to confirm this data (figures 7(a) and (c)), obtaining the same outcome in both measurements—the spin splitting of the 1D subbands is highly anisotropic due to the strong spin–orbit coupling.

The 0.7 structure, which can be seen weakly in figure 7(a), and more strongly after thermal cycling in figure 7(c), is also relatively unaffected by the parallel magnetic field. Since the higher 1D subbands show a highly anisotropic Zeeman spin splitting, the observation that the 0.7 structure shares this anisotropy strongly suggests that this feature is spin related.

4.2. The zero bias anomaly in hole quantum wires

We now turn to the non-equilibrium properties of the 0.7 structure, with the application of a finite dc source–drain bias V_{SD}. In electron systems it has been shown that the 0.7 structure is accompanied by an enhanced conductance at zero source–drain bias, which falls away rapidly as the magnitude of the source–drain bias is increased [27]. The resulting conductance peak at $V_{SD} = 0$ is a characteristic signature of an anomaly in the density of states at the Fermi energy, and shares many of the features of the zero bias anomaly (ZBA) observed in quantum dots: it is suppressed by increasing the temperature and by an in-plane magnetic field. This has lead to suggestions that the 0.7 structure arises from a Kondo-like correlated state, where an electron is localized in the wire [5, 6], although very recently it has been suggested that the Kondo-like behaviour and the 0.7 feature are separate effects in electron quantum wires [28].

In figure 8 we investigate the zero bias anomaly observed in the T483 quantum wire [29]. Figure 8(a) shows the

[7] We limit our analysis to low magnetic fields, as the magnetic length becomes very small at higher B, and bandstructure effects become more complex.

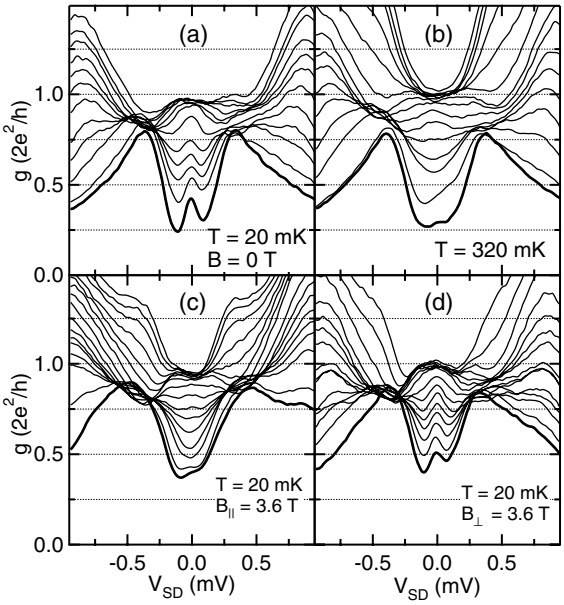

Figure 8. The zero bias anomaly (ZBA) in a hole quantum wire. (a) The differential conductance is plotted as a function of applied source–drain bias, for different values of V_{SG}. (a) At $B = 0$ and $T = 20$ mK a clear peak is seen around $V_{SD} = 0$, highlighted by the bold trace. (b) Increasing the temperature to 320 mK suppresses the ZBA. (c) An in-plane magnetic field of 3.6 T lifts the spin degeneracy and also kills the ZBA peak. (d) In contrast a perpendicular magnetic field of 3.6 T does not lift the spin degeneracy, and the ZBA remains.

differential conductance as a function of source–drain bias for several different values of the side-gate bias V_{SG}. A clear peak centred around $V_{SD} = 0$ is seen for conductances below $2e^2/h$, as indicated by the bold trace. Increasing the temperature to $T = 320$ mK eliminates the ZBA (figure 8(b)), which is much more sensitive to temperature than the ZBA observed in electron samples [27].

We can use the anisotropic spin splitting of the 1D hole subbands to test whether the zero bias anomaly is spin related, and whether it has the same anisotropy as the 0.7 structure. Figure 8(c) shows the effect of a 3.6 T parallel magnetic field on the zero bias anomaly. This field lifts the spin degeneracy of the 1D subbands, and suppresses the ZBA. However if the same magnetic field is applied perpendicular to the quantum wire, as shown in figure 8(d), the Zeeman splitting of the integer 1D subbands is much weaker, and we find that the ZBA is still present. These results strongly suggest that the destruction of the zero bias anomaly is spin related, and that the ZBA and 0.7 structure are intimately related.

5. Summary

In summary, we have studied the 0.7 structure and zero bias anomaly in high quality hole quantum wires. Interaction effects should be much stronger in these systems, because of the enhanced hole effective mass. Yet the zero magnetic field data for electron and hole quantum wires are strikingly similar, with a clear 0.7 structure that becomes stronger with increasing temperature. However unlike 1D electron systems the Zeeman splitting caused by an in-plane magnetic field is highly anisotropic for 1D holes, due to the strong spin–orbit coupling. We have shown that both the 0.7 structure and the ZBA share this anisotropic response to an in-plane magnetic field. These results suggest that the 0.7 structure and the ZBA are directly linked, and that they are both related to spin.

Our data also provide new constraints to test several of the proposed models for the 0.7 structure. Firstly, since the phonon coupling is very different for holes and electrons, it is unclear whether models involving acoustic phonon scattering can explain the data both in electrons and holes [4]. Secondly, it is not obvious that the Kondo model [5] can be applied to hole systems when only the $m_J = 3/2$ band is occupied. More work is needed to understand the electronic and spin properties of holes confined to 1D systems, but already it is clear that 1D holes have unusual spin properties with no counterpart in spin-1/2 electron systems.

Acknowledgments

We thank U Zülicke for many enlightening discussions, and J W Cochrane for technical support. This work was funded by the ARC and EPSRC. ARH acknowledges an ARC Professorial Fellowship, RD and APM acknowledge ARC Postdoctoral Fellowships, and MYS acknowledges an ARC Federation Fellowship.

References

[1] van Wees B J, van Houten H, Beenakker C W J, Williamson J G, Kouwenhoven L P, van der Marel D and Foxon C T 1988 Quantized conductance of point contacts in a two-dimensional electron gas *Phys. Rev. Lett.* **60** 848–50

[2] Wharam D A, Thornton T J, Newbury R, Pepper M, Ahmed H, Frost J E F, Hasko D G, Peacock D C, Ritchie D A and Jones G A C 1988 One-dimensional transport and the quantization of the ballistic resistance *J. Phys. C: Solid State Phys.* **21** L209–14

[3] Thomas K J, Nicholls J T, Simmons M Y, Pepper M, Mace D R and Ritchie D A 1996 Possible spin polarization in a one-dimensional electron gas *Phys. Rev. Lett.* **77** 135–8

[4] Seelig G and Matveev K A 2003 Electron–phonon scattering in quantum point contacts *Phys. Rev. Lett.* **90** 176804

[5] Meir Y, Hirose K and Wingreen N S 2002 Kondo model for the '0.7 anomaly' in transport through a quantum point contact *Phys. Rev. Lett.* **89** 196802

[6] Hirose K, Meir Y and Wingreen N S 2003 Local moment formation in quantum point contacts *Phys. Rev. Lett.* **90** 26804

[7] Winkler R 2003 *Spin–Orbit Coupling Effects in Two-Dimensional Electron and Hole Systems* (Berlin: Springer)

[8] Zailer I, Frost J E F, Ford C J B, Pepper M, Simmons M Y, Ritchie D A, Nicholls J T and Jones G A C 1994 Phase coherence, interference, and conductance quantization in a confined two-dimensional hole gas *Phys. Rev.* B **49** 5101

[9] Daneshvar A J, Ford C J B, Hamilton A R, Simmons M Y, Pepper M and Ritchie D A 1997 Enhanced g factors of a one-dimensional hole gas with quantized conductance *Phys. Rev.* B **55** 13409–12

[10] Rokhinson L P, Pfeiffer L N and West K W 2006 Spontaneous spin polarization in quantum point contacts *Phys. Rev. Lett.* **96** 156602

[11] Winkler R 2004 Spin density matrix of spin-3/2 hole systems *Phys. Rev.* B **70** 125301
[12] Csontos D and Zülicke U 2007 Large variations in the hole spin splitting of quantum-wire subband edges *Phys. Rev.* B **76** 73313
[13] Csontos D and Zülicke U 2007 Quantum confinement effects on the spin splitting and polarization dependence of quasi-1D holes *Physica* E at press
[14] Zülicke U 2006 Electronic and spin properties of hole point contacts *Phys. Status Solidi* c **3** 4354–8
[15] Clarke W R, Micolich A P, Hamilton A R, Simmons M Y, Muraki K and Hirayama Y 2005 Fabrication and characterization of a 2D hole system a in novel (311)A GaAs SISFET *Microelectron. J.* **36** 327–30
[16] Klochan O, Clarke W R, Danneau R, Micolich A P, Ho L H, Hamilton A R, Muraki K and Hirayama Y 2006 Ballistic transport in induced one-dimensional hole systems *Appl. Phys. Lett.* **89** 092105
[17] Danneau R, Clarke W R, Klochan O, Micolich A P, Hamilton A R, Simmons M Y, Pepper M and Ritchie D A 2006 Conductance quantization and the $0.7 \times 2e^2/h$ conductance anomaly in one-dimensional hole systems *Appl. Phys. Lett.* **88** 012107
[18] Castleton I M, Davies A G, Hamilton A R, Frost J E F, Simmons M Y, Ritchie D A and Pepper M 1998 Closely separated one-dimensional wires: coupled ballistic conduction, wave function hybridization and compressibility investigations *Physica* B **251** 157–61
[19] Hamilton A R, Klochan O, Danneau R, Clarke W R, Ho L H, Micolich A P, Simmons M Y, Pepper M, Ritchie D A, Muraki K and Hirayama Y 2008 Quantum transport in one-dimensional GaAs hole systems *Int. J. Nanotechnol.* **5** 318–30
[20] Danneau R, Clarke W R, Klochan O, Ho L H, Micolich A P, Hamilton A R, Simmons M Y, Pepper M and Ritchie D A 2006 Ballistic transport in one-dimensional bilayer hole systems *Physica* E **34** 550–2
[21] Thomas K J, Nicholls J T, Appleyard N J, Simmons M Y, Pepper M, Mace D R, Tribe W R and Ritchie D A 1998 Interaction effects in a one-dimensional constriction *Phys. Rev.* B **58** 4846–52
[22] Reilly D J, Buehler T M, O'Brien J L, Hamilton A R, Dzurak A S, Clark R G, Kane B E, Pfeiffer L N and West K W 2002 Density-dependent spin polarization in ultra-low-disorder quantum wires *Phys. Rev. Lett.* **89** 246801
[23] Pyshkin K S, Ford C J B, Harrell R H, Pepper M, Linfield E H and Ritchie D A 2000 Spin splitting of one-dimensional subbands in high quality quantum wires at zero magnetic field *Phys. Rev.* B **62** 15842–50
[24] Hamilton A R, Frost J E F, Smith C G, Kelly M J, Linfield E H, Ford C J B, Ritchie D A, Jones G A C, Pepper M, Hasko D G and Ahmed H 1992 Back-gated split-gate transistor: a one-dimensional ballistic channel with variable Fermi energy *Appl. Phys. Lett.* **60** 2782
[25] Thomas K J, Simmons M Y, Nicholls J T, Mace D R, Pepper M and Ritchie D A 1995 Ballistic transport in one-dimensional constrictions formed in deep two-dimensional electron gases *Appl. Phys. Lett.* **67** 109–11
[26] Danneau R, Klochan O, Clarke W R, Ho L H, Micolich A P, Simmons M Y, Hamilton A R, Pepper M, Ritchie D A and Zulicke U 2006 Zeeman splitting in ballistic hole quantum wires *Phys. Rev. Lett.* **97** 026403
[27] Cronenwett S M, Lynch H J, Goldhaber-Gordon D, Kouwenhoven L P, Marcus C M, Hirose K, Wingreen N S and Umansky V 2002 Low-temperature fate of the 0.7 structure in a point contact: a Kondo-like correlated state in an open system *Phys. Rev. Lett.* **88** 226805
[28] Sfigakis F, Ford C J B, Pepper M, Kataoka M, Ritchie D A and Simmons M Y 2008 Kondo effect from a tunable bound state within a quantum wire *Phys. Rev. Lett.* **100** 026807
[29] Danneau R, Klochan O, Clarke W R, Ho L H, Micolich A P, Simmons M Y, Hamilton A R, Pepper M and Ritchie D A 2008 0.7 structure and zero bias anomaly in ballistic hole quantum wires *Phys. Rev. Lett.* **100** 016403